Engineering supramolecular forming proteins to chelate heavy metals for waste water remediation

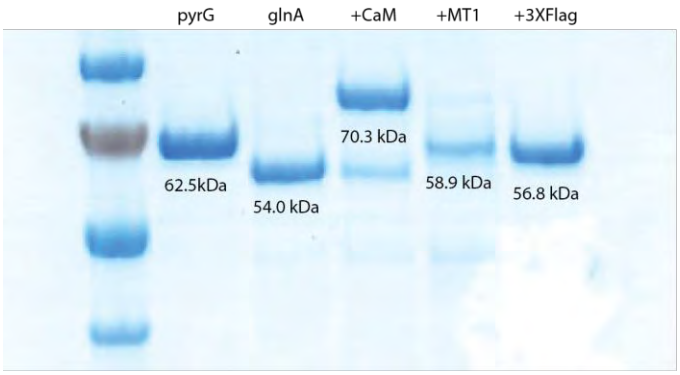

Supplementary Figure 1 | Examining protein expression and purity using SDS-PAGE and Coomassie staining. Purified pyrG, glnA, +CaM, +MT1, and +3XFlag showed the correct band size. Only +CaM showed a fainter second band which corresponds to the unfused glnA, suggesting that a fraction of the +CaM fusion was cleaved either during expression or during the purification process.

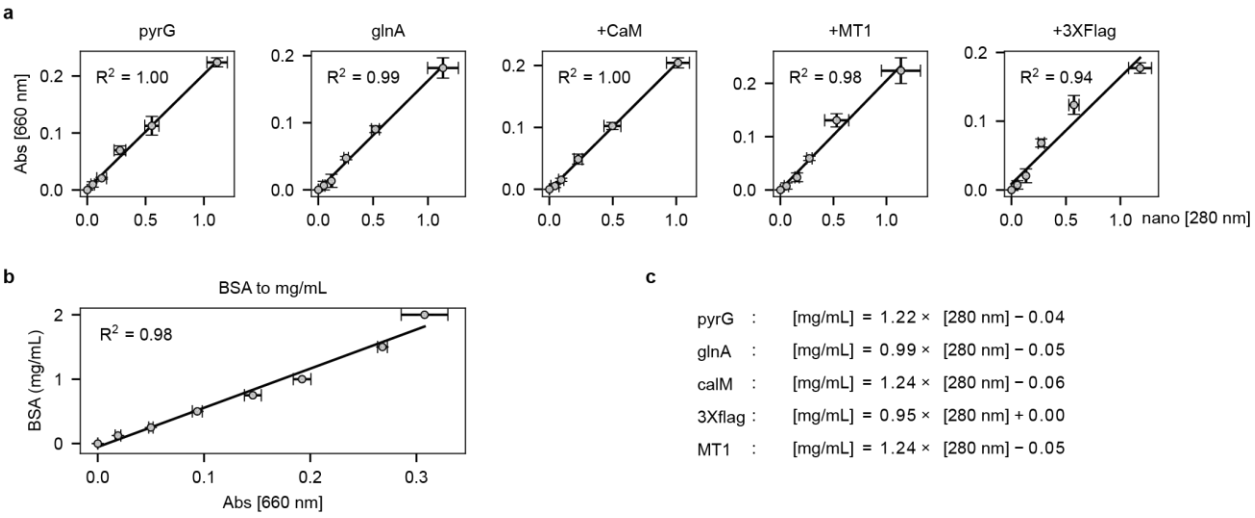

Supplementary Figure 2 | Protein concentrations measured on Nanodrop correlated with Pierce 660 Protein Assay. a) Serial dilutions of proteins pyrG, glnA, +CaM, +MT1, and +3XFlag were measured on Nanodrop (x-axis) and Pierce 660 nm protein assay (y-axis). **b**) Pierce assay was then used to create a calibration curve against BSA standards. The calibration curve, as well as the relationship between the Nanodrop and Pierce 660 nm protein assay was used to create a linear relationship **c**) to better quantify concentrations for each protein. For all data, the mean ± s.d. of three replicates are shown.

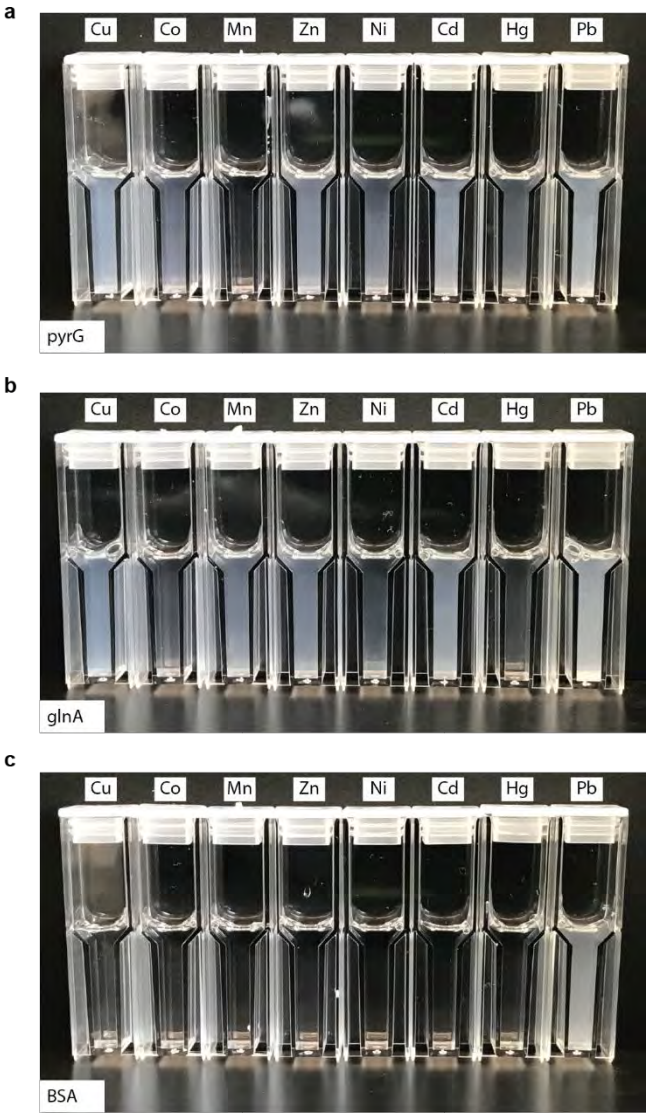

Supplementary Figure 3 | Images of 100 μM pyrG, glnA and BSA mixed with 1 mM of metals. a) pyrG mixed with 100 μM metal labelled on the top showed aggregation visible by opaqueness and change in color due to metal chelation. **b**) A similar trend is shown for glnA. **c**) BSA was used as a control to differentiate protein aggregation due to protein denaturation or metal precipitation. Pb was the only metal to show a visible change in opacity, as it is known to favorably form hydroxides in neutral pH over time.

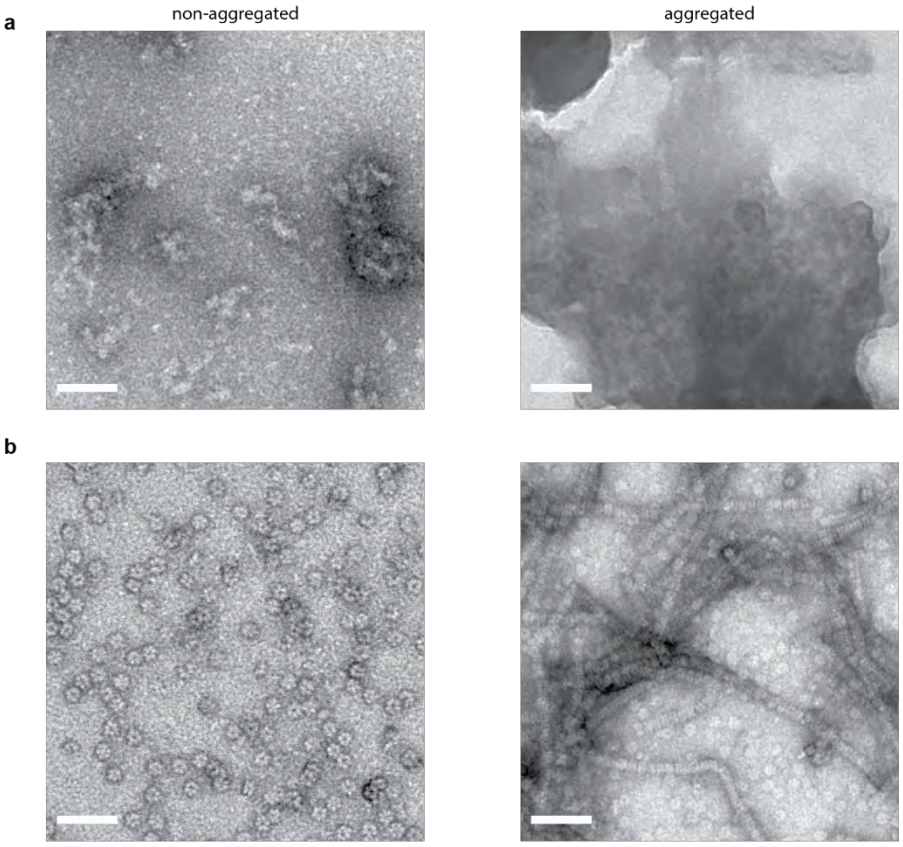

Supplementary Figure 4 | HRTEM images of pyrG and glnA. a) Purified pyrG showed no definitive structure, but rather monomers that sometimes formed small aggregates. When aggregated, pyrG produced densely packed structures as seen by dark contrast under TEM. **b**) glnA formed the predicted structure of two hexamers stacked on top of one another. When aggregated, glnA formed chain-like structure. Scale bars represent 50 nm for all images.

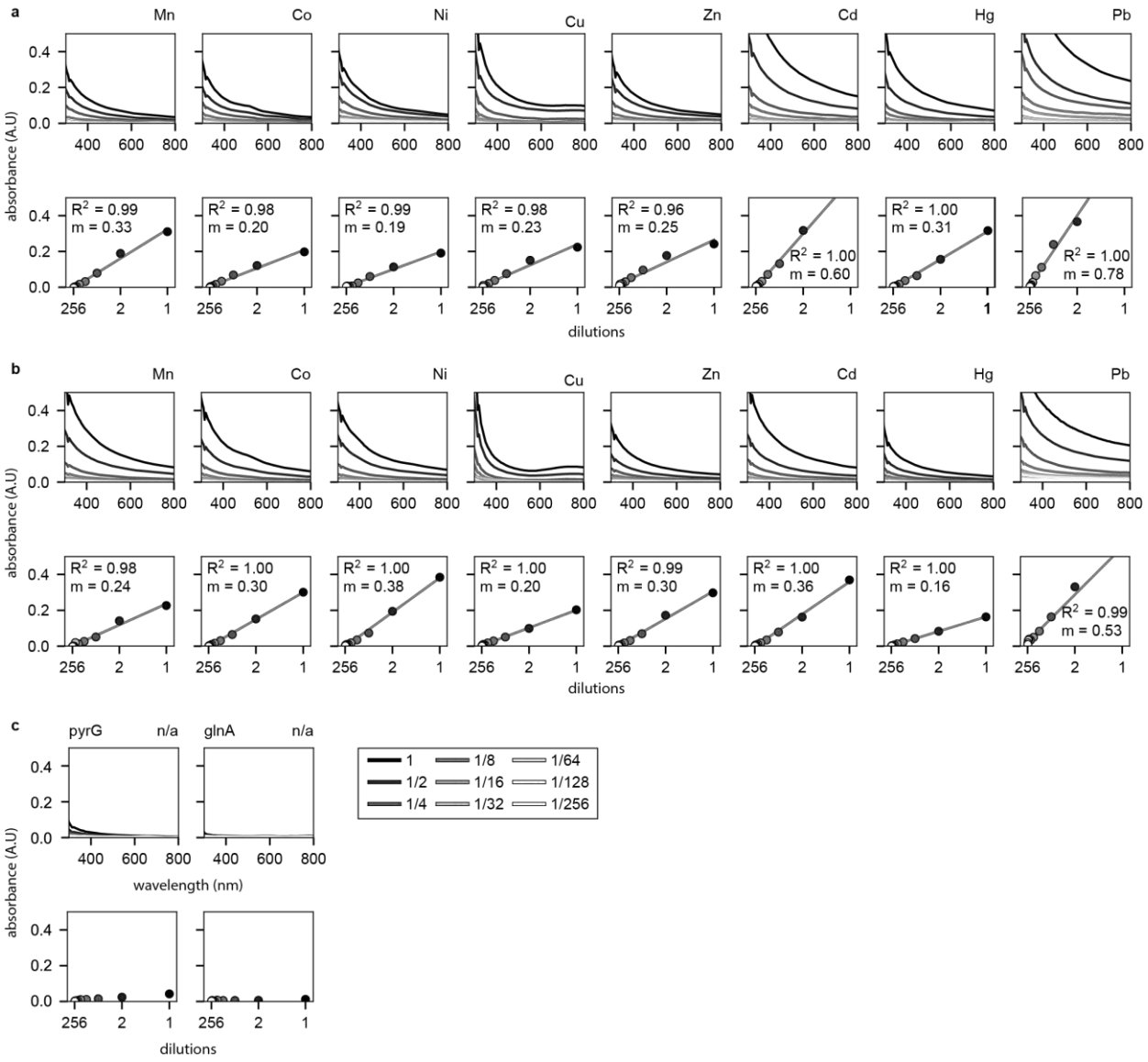

Supplementary Figure 5 | Absorbance scans of pyrG and glnA at varying degrees of metal-induced aggregation. a, b) pyrG and glnA absorbance scans for all metals tested in this study at increasing dilutions as indicated by the lower panel x-axis and increasing line opacity. Scans at 350 nm gave a linear relationship with good signal to noise for the various dilutions of protein aggregation. **c**) Absorbance scans of non-aggregated pyrG and glnA absent of any metals.

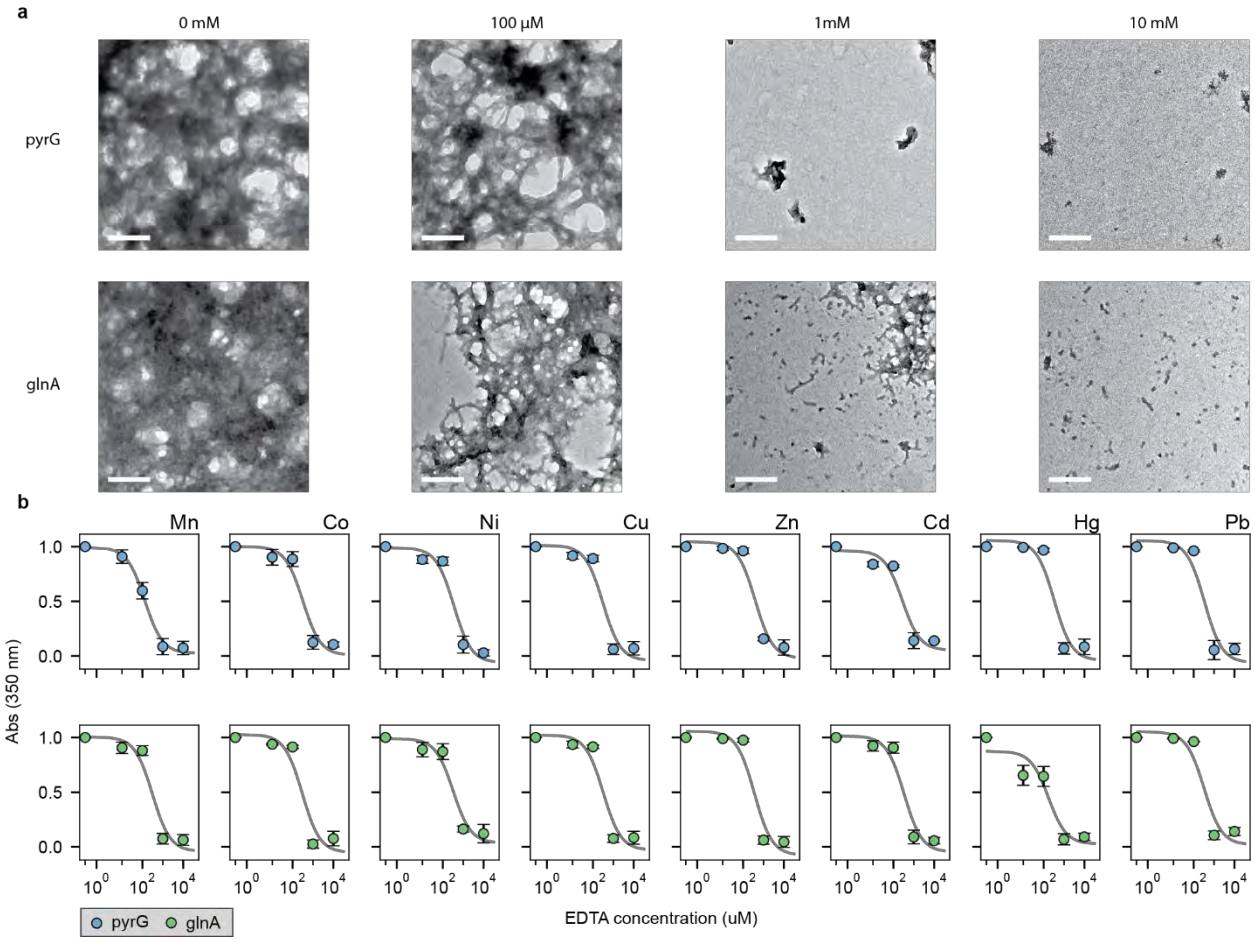

Supplementary Figure 6 | Reversibility of aggregated pyrG and glnA at varying EDTA concentrations. a) Top/bottom row are pyrG and glnA, respectively. Columns represent concentrations of EDTA added after 100 μM of protein was aggregated with 1 mM of Zn for 1 hour. Scale bars represent 200 nm for all images. **b**) After protein aggregation, concentrations of EDTA (x-axis) were added to outcompete metal binding and dissociate protein subunits. The intensity of aggregation was measured at 350 nm after adding EDTA for 10 min. For all data, the mean $\pm$ s.d. of three replicates are shown.

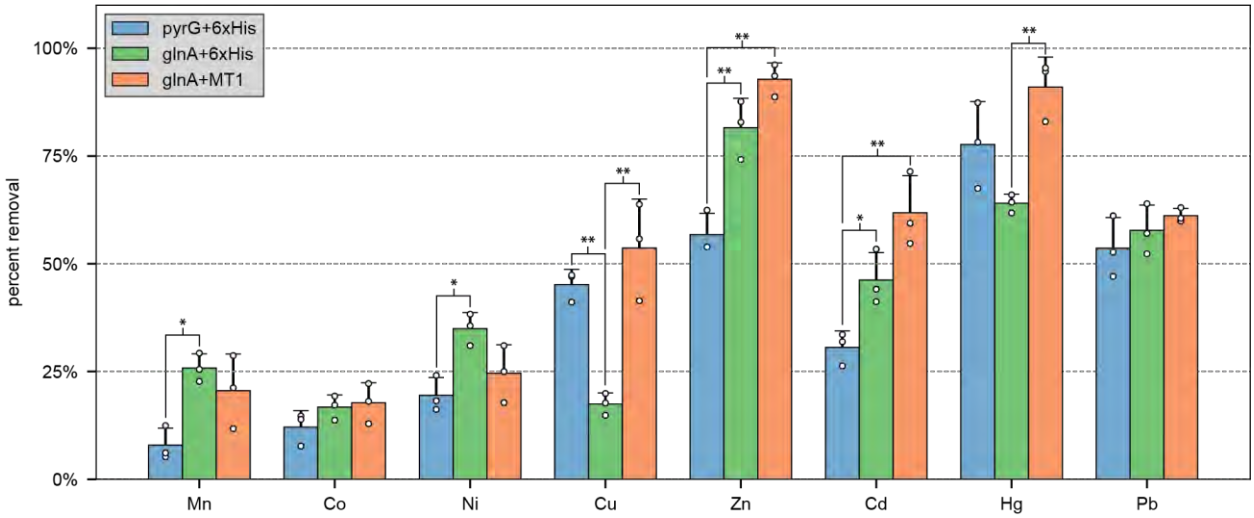

Supplementary Figure 7 | Percent metal removal for multi-metal experiments using pyrG, glnA, and glnA +MT1. Multi-metal removal data reported in Error! Reference source not found.**c,d** and Error! Reference source not found.**e** were converted to percent fraction of metal removed. For all data, the mean ± s.d. of three replicates are shown.

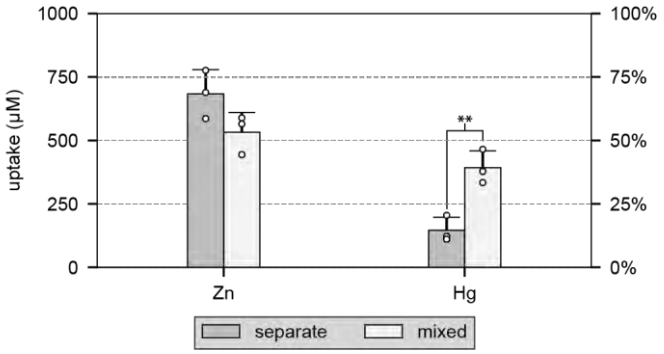

Supplementary Figure 8 | Mixing Zn and Hg alters glnA metal removal capacities. Individually, Zn is removed significantly more than Hg when mixed with 100 μM glnA fused to a 6xHis tag. However, when Zn and Hg are mixed together, Zn removal decreases while Hg increases ($p < .05$). An explanation for this trend is that glnA does not aggregate as strongly with Hg as it does with Zn. However, when mixed together, glnA aggregates in the presence of Zn but the 6xHis tag preferentially pulls down Hg over Zn. Therefore, Hg removal piggy-backs Zn aggregation of glnA.

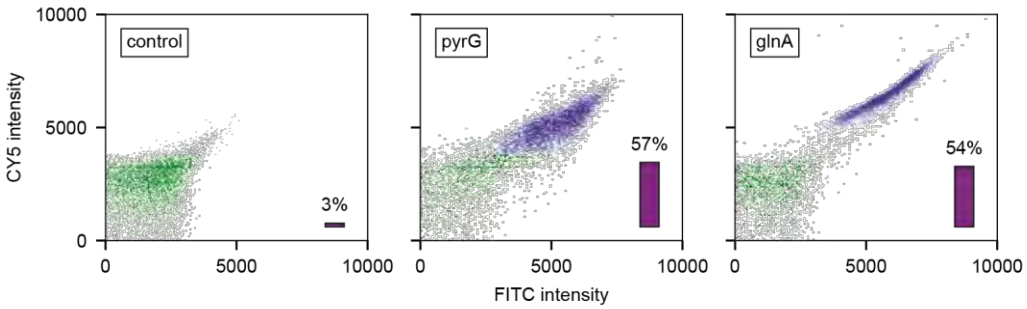

Supplementary Figure 9 | Yeast display of pyrG and glnA monomers using EBY100 and pYD1 vector. Expression was analyzed using flow cytometry by staining the N'-terminus HA tag and C'-terminus Flag tag with antibodies conjugated with 488 (FITC) and 647 (Cy5) dyes. A control was measured in parallel to properly bin the population of expressing cells.

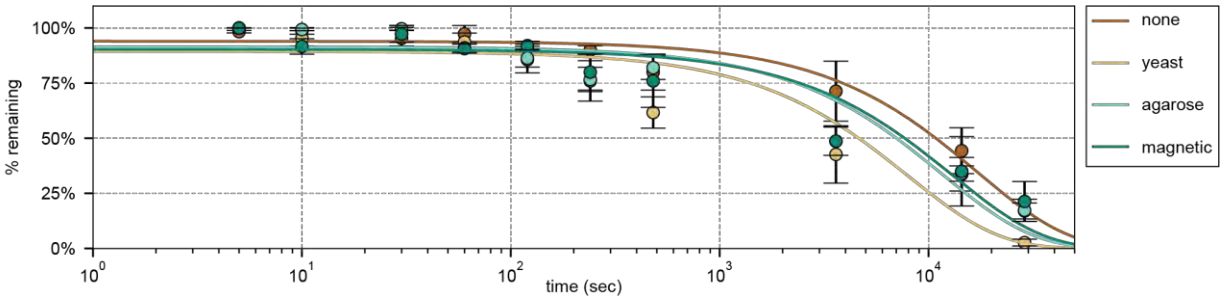

Supplementary Figure 10 | Sedimentation study of non-fused glnA with agarose or magnetic beads, or yeast as controls. glnA without a 3XFlag tag was aggregated and mixed with anti-flag agarose or magnetic beads. The yeast control had EBY100 strains transformed with an empty pYD1 vector and mixed with aggregated glnA. Overall, glnA sedimentation rates for each control largely remained unchanged. For all data, the mean ± s.d. of three replicates are shown.

name	direction	sequence
pyrG	fwd	CAGCAGCGGCGAAAACCTGTATTTTCAGAGCACAACGAACTATATTTTTGTGACC
	rev	CCACCAGTCATGCTAGCCATATGTTACTTCGCCTGACGTTT
glnA	fwd	CAGCAGCGGCGAAAACCTGTATTTTCAGAGCTCCGCTGAACACGTAC
	rev	CCACCAGTCATGCTAGCCATATGTTAGACGCTGTAGTACAGC
pET28c(+)	fwd	ACAGGTTTTCGCCGCTGCTGTGATGATG
	rev	CATATGGCTAGCATGACTGGTG

Supplementary Table 1 | Primers to amplify pyrG and glnA from *E. coli* genomic DNA. 5' fwd primer contain a 6xHis tag and TEV protease site that is added upstream to the gene. Purified PCR products were then assembled using Gibson assembly into pET28c(+) linearized by the primers shown.

name	direction	sequence
+CaM	fwd	CGGCGAAAACCTGTATTTTCAGAGCTCCTCCAATCTTACCGAAG
	rev	CGGAGCCGCTACCGCCTTTAGATAACAAAGCAGCGA
+MT1a	fwd	CGGCGAAAACCTGTATTTTCAGAGCATGGCTGATTCTAATTGTGG
	rev	CGGAGCCGCTACCGCCACAATTACAGTTTGAACCACAA
glnA (bB)	fwd	GGCGGTAGCGGCTCCGCTGAACACGTACT
	rev	GCTCTGAAAATACAGGTTTTCG

Supplementary Table 2 | Calmodulin (CaM) and plant metallothionein (MT1a) primers to construct glnA fusions in pET28c(+). CaM was isolated from yeast genomic DNA, whereas MT1a was codon-optimized and isolated from a synthesized plasmid. Primers contain the appropriate overhangs insert into the constructed pET28c(+) glnA vector using Gibson assembly.

name	direction	sequence
+3XFlag	fwd	CATGACATCGATTACAAGGATGACGATGACAAGTCCGCTGAACACGTACT
	rev	ATCTTTATAATCACCGTCATGGTCTTTGTAGTCGCTCTGAAAATACAGGTTTTCG

Supplementary Table 3 | Primers used to fuse a 3XFlag tag into the constructed pET28c(+) glnA vector. Primers were used to linearize the pET28c(+) vector with each primer overhang encoding half of the 3XFlag sequence. Linearized product was then blunt-end ligated to re-circularize the plasmid.

name	direction	sequence
glnA	fwd	GCTAGCTCAGCCGAACACGTATTAAC
	rev	GGATCCAACTGAGTAATACAATTCAAATTCAAC
pyrG	fwd	GCTAGCACAACGAACTATATTTTTGTGACc
	rev	GGATCCCTTCGCCTGACGTTTCTG

Supplementary Table 4 | Primers used to insert bacterial glnA and pyrG genes into pYD1 yeast display vector. Primers were used to amplify glnA and pyrG with NheI and BamHI overhangs using PCR. The pYD1 vector was cut with NheI and BamHI and ligated with the digested pyrG or glnA product.